

# Investigation of low-angle laser light scattering patterns using the modified Twomey iterative method for particle sizing

Tatsuo Igushi<sup>1,a)</sup> and Hideto Yoshida<sup>2</sup>

<sup>1</sup>Horiba, Co., Ltd., Miyanohigashi, Kisshoin, Minami-ku, Kyoto 601-8510, Japan

<sup>2</sup>Department of Chemical Engineering, Hiroshima University, 1-4-1, Kagamiyama, Higashi-Hiroshima 739-8527, Japan

(Received 10 August 2010; accepted 3 November 2010; published online 31 January 2011)

We first applied the Twomey iteration method to the low-angle laser light scattering (LALLS) method. The Twomey method is known by the simple iteration algorithm for Fredholm integral equation. However, the algorithm is not applied to the LALLS result itself because the kernel function pattern is not stable. We solved the unstable kernel issue by modifying the Twomey algorithm to fit the LALLS data in this study. The performance of inversion was studied by computer simulation and experimental results from detectors containing 24 elements from angle 0.0005 to 2.5 rad. The computer simulation was carried out for particles of mean sizes from 0.1 to 1000  $\mu\text{m}$  with mono-dispersion and log-normal distributions. A conventional algorithm is also carried out to compare the performance of the Twomey method. The noise effect of the inverse problem was tested by computer simulation. Experimental results were measured with standard polystyrene latex from 0.081 to 1007  $\mu\text{m}$ . All the tests were performed under conditions in which the light from a linearly polarized laser at 633 nm was scattered by a diluted aqueous suspension. The modified Twomey (MT) method and conventional method show good reproduction results for particles with log-normal distributions. However, narrow distribution particles indicate that the MT method shows excellent reproduction results when compared with the conventional method. © 2011 American Institute of Physics. [doi:10.1063/1.3520136]

## I. INTRODUCTION

The majority of powdered substances used in modern industry have a polydisperse distribution. This includes most of the representative powders used in fine ceramics and in the source of cement, as well as in the food industry, medicine, and chemistry. Conventional measurement methods include imaging, filtering, centrifugal sedimentation, the electrical sensing zone method, and x-ray sedimentation. Among the measurement methods now in use, the laser scattering method is currently the most popular method because it is simple, precise, and relatively fast. In some cases, the results of analysis can be completely different, depending on the type of measurement equipment used. Then, it is important to increase the reliability of the data. The most stringent condition required for evaluating the performance of a particle size distribution measurement device is in the reproducibility of its distribution analysis. There are several methods available for measuring particle size distribution of the larger diffraction method.<sup>1-3</sup>

Low-angle laser light scattering (LALLS) is one of the most useful techniques for measuring particle size distribution due to the wide dynamic range of measurement, good repeatability, and easy operation. The relationship between the particle size and the light scattering intensity at each angle is expressed by the Fredholm integral equation of the first kind. When the particle size distribution is known, the scattering intensity pattern can be calculated. However, when

the particle size distribution is not known, observed intensity of the scattering pattern must be solved by an inversion method. In order to solve an inversion problem, the parametric approach<sup>4-6</sup> and nonparametric approach can be considered. As the nonparametric approach can achieve particle size distribution without a prior distribution message, researchers are becoming increasingly carried out in studying and adopting these methods.<sup>7,8</sup>

The conventional method, as proposed by Philips-Twomey,<sup>9</sup> and the iterative method, as proposed by Chahine,<sup>10,11</sup> are two common algorithms. The advantage of the Philips-Twomey method is its computational speed and its ability to handle many size classes with stability. On the other hand, the result is smoothed and thus resolution is sacrificed. The Chahine scheme has fast convergence, but the result is noise sensitive and the number of sensors and the number of size classes should be equal. Twomey<sup>9</sup> improved the iteration algorithm to improve the limitation of Chahine's method. The iterative method proposed by Twomey has been applied to the analysis of data from indirect measurement techniques that include backscattered spectrums, multi-wavelength extinction coefficient measurements, cascade impactors, the diffusion battery, and electrical aerosol size analyzer measurements in aerosol science.<sup>12-15</sup> However, the application of this approach to retrieve particle size distribution from the LALLS has not been explored.

In this study, the improved Twomey iterative method was applied to the LALLS method. We report on the extensive tests of Twomey using computer simulations of the LALLS patterns over the scattering angle ranges. Conditions of the computer simulations are 24 elements of sensors from

<sup>a)</sup>Electronic mail: tatsuo.igushi@horiba.com. Telephone: +81-75-325-5035. Fax: +81-75-315-4851.

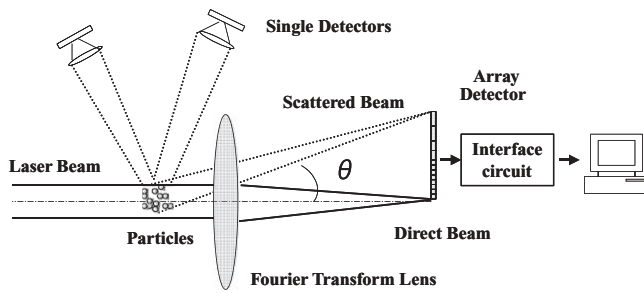


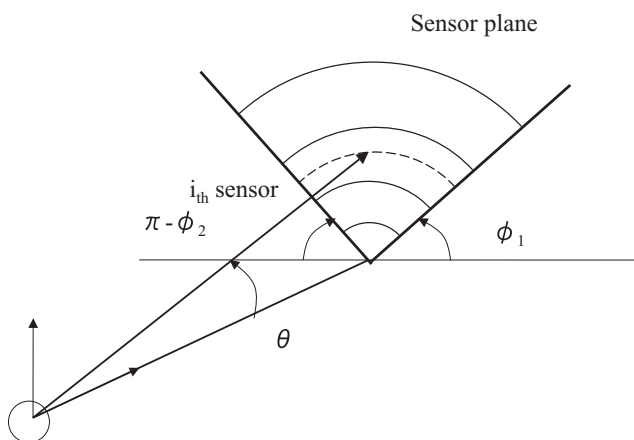
FIG. 1. Schematic layout of LALLS particle size distribution analyzer.

0.03° to 150° generated from both monodispersed and poly-dispersed distribution. The same simulation with the conventional method was used to validate the numerical procedure of the iteration method. Experimental results are also obtained with the iterative method. Comparing the calculated results between the improved Twomey method and the conventional method, the new important conclusions are obtained.

## II. INVERSION METHODS

The particles cause the light to scatter in all directions, but by using a Fourier transform lens, it is possible to concentrate light that has been scattered in the same angular direction as shown in Fig. 1. Scattering from a single spherical scatter illuminated by a collimated laser beam gives rise to an angular variation of the intensity in the far field<sup>10,16,17</sup> as shown in Fig. 2. The shape of the array detector has a concentric ring structure because the shape of the particles is assumed to be spherical when calculated by the Mie theory. Each detector has a finite dimension, covering an angular range  $\Delta\theta$  and  $\Delta\phi$ . The value of  $\Delta\theta$  and  $\Delta\phi$  depends on the radial location of the detector. The total scattering intensity detected at the average scattering angles  $\theta$  and  $\phi$  from particles in the scattering volume per unit detector area is expressed by the Fredholm integral equation of the first kind in Eq. (1),

$$g(\theta, \phi, D) = \int_{D_{\min}}^{D_{\max}} K(\theta, \phi, D) f(D) dD, \quad (1)$$

FIG. 2. Geometry of array detector. Schematic of a regular array sensor for LALLS. The array sensor plane is divided into a fan-shaped ring. Each of sensors is eliminated by polar angle  $\phi_1$  and  $\phi_2$ , and scattering angle  $\theta$ .

$K(\theta, \phi, D)$  is termed as a kernel function, which is the unit volume scattering intensity from a particle of diameter  $D$ , detected by a unit detector area at angles  $\theta$  and  $\phi$ . In practice, this continuous integration is replaced by a discrete matrix format in order to resolve the size distribution  $f(D_j)$ :

$$g_i = \sum_{j=1}^m K_i(D_j) f(D_j) \Delta D_j \quad (2)$$

or

$$g = Kf, \quad (3)$$

where

$g_i$  is the output from the  $i$ th detector;

$i$  is the number of detector;

$K_i(D_j)$  is the kernel function of the  $i$ th detected scattering intensity;

$D_j$  is the typical particle size;

$j$  is the number of column of diameter;

$f(D_j)$  is the frequency particle size distribution at  $D_j$  based on volume;

$\Delta D_j$  is the interval between particle size distributions;

$M$  is the number of particle size column.

The kernel function was generated by Mie theory with a vertical polarized light of wavelength 633 nm and the relative refractive indices of the particles were 1.19 or 1.33. Because of the symmetry of the scattering pattern, the matrix calculated by Mie theory is independent of  $\phi$ . Thus, in Eq. (2), the variable  $\phi$  has been removed. Therefore, it becomes a simple matter to calculate the detector output by using the kernel function. The log-normal distributions with various standard deviations are used to generate particle size distribution. Nevertheless, the value we can obtain experimentally is only the detector output, and what we are concerned with in this paper is how to inverse the particle size distribution from the experimentally obtained detector output.

## III. CONVENTIONAL METHOD

An algorithm of the conventional method to obtain the particle size distributions is frequently used in LALLS instruments.<sup>8,9</sup> The conventional method is obtained by minimizing Eqs. (4a) and (4b) through a least square algorithm, with the constraints being that the distribution is represented by non-negative numbers only. It is also a smooth function that goes to zero at the extremities of the chosen size range:

$$J = (Kf - g)^T (Kf - g) + \gamma f^T H f, \quad (4a)$$

$$\frac{\partial J}{\partial f} = 0, \quad (4b)$$

$$f = (K^T K + \gamma H)^{-1} K^T g, \quad (5)$$

where the superscript  $T$  denotes the transposition,  $\gamma$  is the regularization parameter that determines the degree of smoothing, and  $H$  contains smoothing instructions. These effectively link the elements of  $J$  by their second-order differences or other constraints by filtering both experimental and approximation errors. By applying the well-known Lagrange's

method of undetermined multipliers, we can obtain a set of equations for determining the particle size distribution. The residue square  $R^2$  is calculated by Eq. (6):

$$R^2 = \sum_{i=1}^n \left( g_i - \sum_{j=1}^m [K_i(D_j) f(D_j)] \right)^2. \quad (6)$$

#### IV. MODIFIED TWOMEY (MT) ITERATION METHOD

An improved algorithm of the nonlinear iteration method is based on the Twomey scheme by using Eq. (2). Particle size distribution  $f(D_j)$  should be positive. Therefore, a correction function should be less than 1 to be guaranteed positive value of  $f(D_j)$  by the Twomey method. We shall assume that the initial value of the particle size distribution is a constant, in the sense that no restrictive conditions have been applied. The kernel function  $K_i(D_j)$  in Eq. (2) is computed according to Mie theory.<sup>8,18</sup> The numerical value of  $K_i(D_j)$  is changed logarithmically when scattering angles and particle sizes are changed logarithmically. Unfortunately, using the raw value of the kernel function results may indicate unstable retrievals, as the kernel function  $K_i(D_j)$  is dominated by a small angle as shown in Fig. 3. To avoid this problem, a normalized function  $S_i$  can be used to modify the inversion process. In particular, retrieving the modified kernel function  $K'_i(D_j)$ :

$$K'_i(D_j) = \frac{K_i(D_j)}{S_i}, \quad (7)$$

where  $S_i$ , the maximum value of  $K_i(D_j)$ , is more stable.

In the Twomey method, errors included in the measured signal are distributed to each particle size by the value of the corresponding function. Therefore, an overfitting at a specific particle diameter may be observed, even if the number of iterations is the same.<sup>19,20</sup> The speed of modification at any diameter depends on the degree of overlap of each kernel function curves. As there are a limited number of detectors, and there is a difference in efficiency of scattering at the particle diameter,

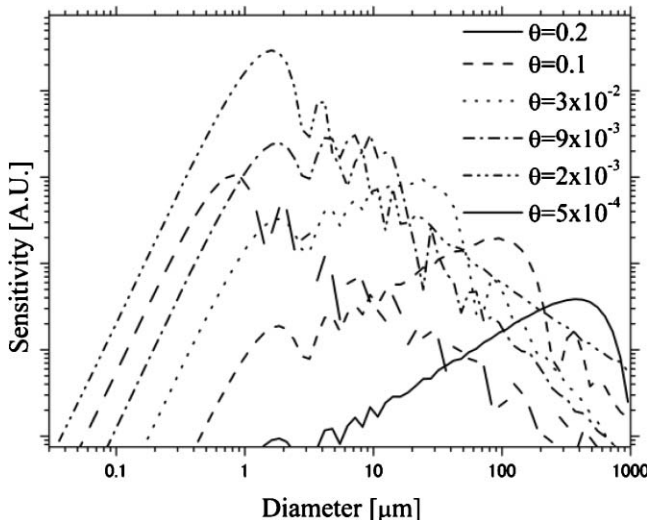


FIG. 3. Examples of the sensitivity of LALLS detectors as a function of the scattering angle  $\theta$  (rad.).

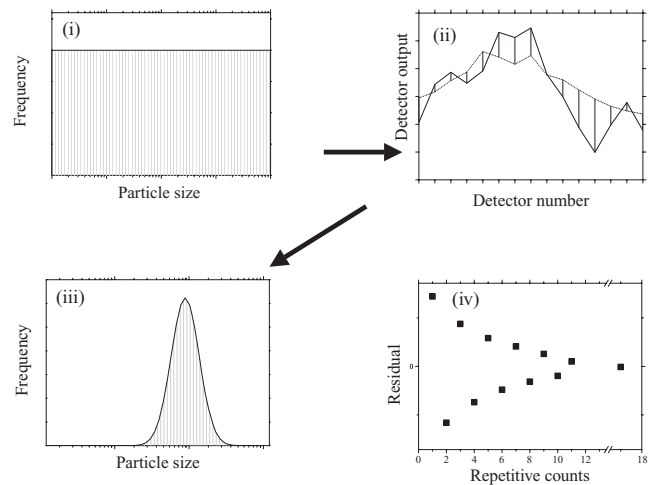


FIG. 4. Schematic flow of particle size distribution by the MT iteration method. Measured detector outputs (solid line) and calculated detector outputs from particle size distribution (dashed line) are shown in part (ii).

the degree of overlap of kernel functions is not flat. In order to avoid the local overfitting issue, we introduce convergent parameters  $M_j$ :

$$M_j = \sum_{i=1}^m K_i(D_j). \quad (8)$$

An algorithm of the MT iteration flow is shown in Fig. 4. First, using the initial value of particle size distribution, we calculate the detector output by Eq. (2). The normalized function  $S_i$  is used to correct particle size distribution.  $M_j$  is then introduced to standardize convergence speed to correct particle size distribution. The correction function calculated by Eq. (9a) is a ratio of the measured and calculated detector output. Using the correction function  $r$ , the first modified particle size distribution is calculated by Eq. (9b). The first modified particle size distribution is not always a good result. Second, the correction function  $r$  is calculated with the measured and calculated detector output from the value of the first modified particle size distribution. Using the second kernel function,  $r$  is used to modify the particle size distribution. The second modified particle size distribution is better than the first modified distribution. The particle size is then modified by the  $r$  value step by step. The modified particle size distribution is then going to have true values:

$$r_i^{k-1} = \frac{\sum_{i=1}^n g_i S_i}{\sum_{i=1}^n \sum_{j=1}^m K'_i(D_j) f^{k-1}(D_j)}, \quad (9a)$$

$$f^k(D_j) = \frac{(r_i^{k-1} - 1) K'_i f^{k-1}(D_j)}{M_j} + f^{k-1}(D_j), \quad (9b)$$

where  $k$  is the number of iteration.

The effect of the convergent parameter  $M_j$  in the iteration is shown in Fig. 5. A single peak of log-normal distribution is used for the computer simulation. Results are simulated by the MT method with flat and weighted value of  $M_j$ . When the weighted  $M_j$  is used, computer simulation results show very good correlation, even if we use

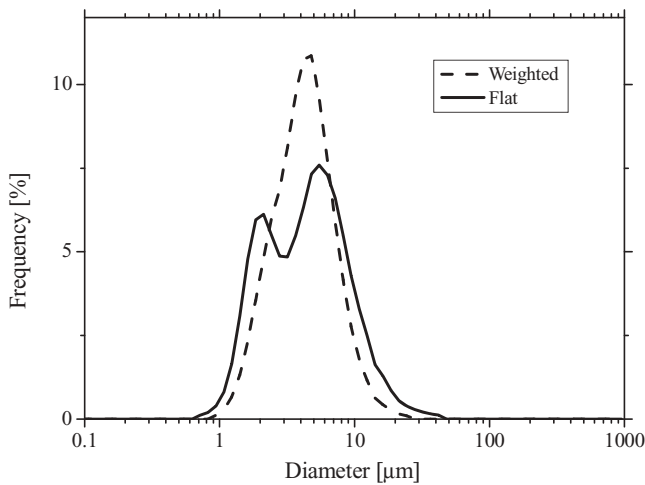


FIG. 5. Example of computer simulation with flat parameter condition (solid line) at single log-normal distribution. For comparison, the normalized parameter results (dashed line) are also plotted.

the same algorithm as shown in Fig. 5.  $M_j$  in Eq. (9) accumulates scattering intensity values at each particle diameter.  $M_j$  is the related scattering cross section. The scattering cross section is known as a vibrational function.<sup>20</sup> However, the value of  $R^2$  by the conventional method was 100 times as large as the MT method at less than  $0.5 \mu\text{m}$  and  $100 \mu\text{m}$  or more.

## V. COMPUTER SIMULATIONS

An evaluation methodology for the analysis process we have introduced is as follows:

- (1) For the particle size distribution  $f(D_j)$ , we assume a log-normal distribution.
- (2) The detector output  $g$  can easily be calculated from the particle size distribution  $f(D_j)$  and the kernel function  $K_i(D_j)$ .
- (3) The only value that can be obtained experimentally is the actual output from the detector. Therefore, using the detector output  $g_i$ , we evaluate the particle size distribution  $f(D_j)$  obtained by the matrix method and the nonlinear iteration method. Evaluative standards used for the particle size distribution  $f(D_j)$  are as follows:
  - (a) A mean diameter often found in particle size distribution,
  - (b) Standard deviation  $\sigma$ ,
  - (c) Values of  $R^2$ .

## VI. RESULTS AND DISCUSSION

We have made a comparison of the results obtained from polydisperse distribution. For the distribution function, we shall use the Gaussian function. We assume a distribution with a mean diameter of  $11.6 \mu\text{m}$  and a standard deviation  $\sigma$  of  $1.0 \times 10^{-1}$  as shown in Fig. 6(a). Figure 6(b) shows the

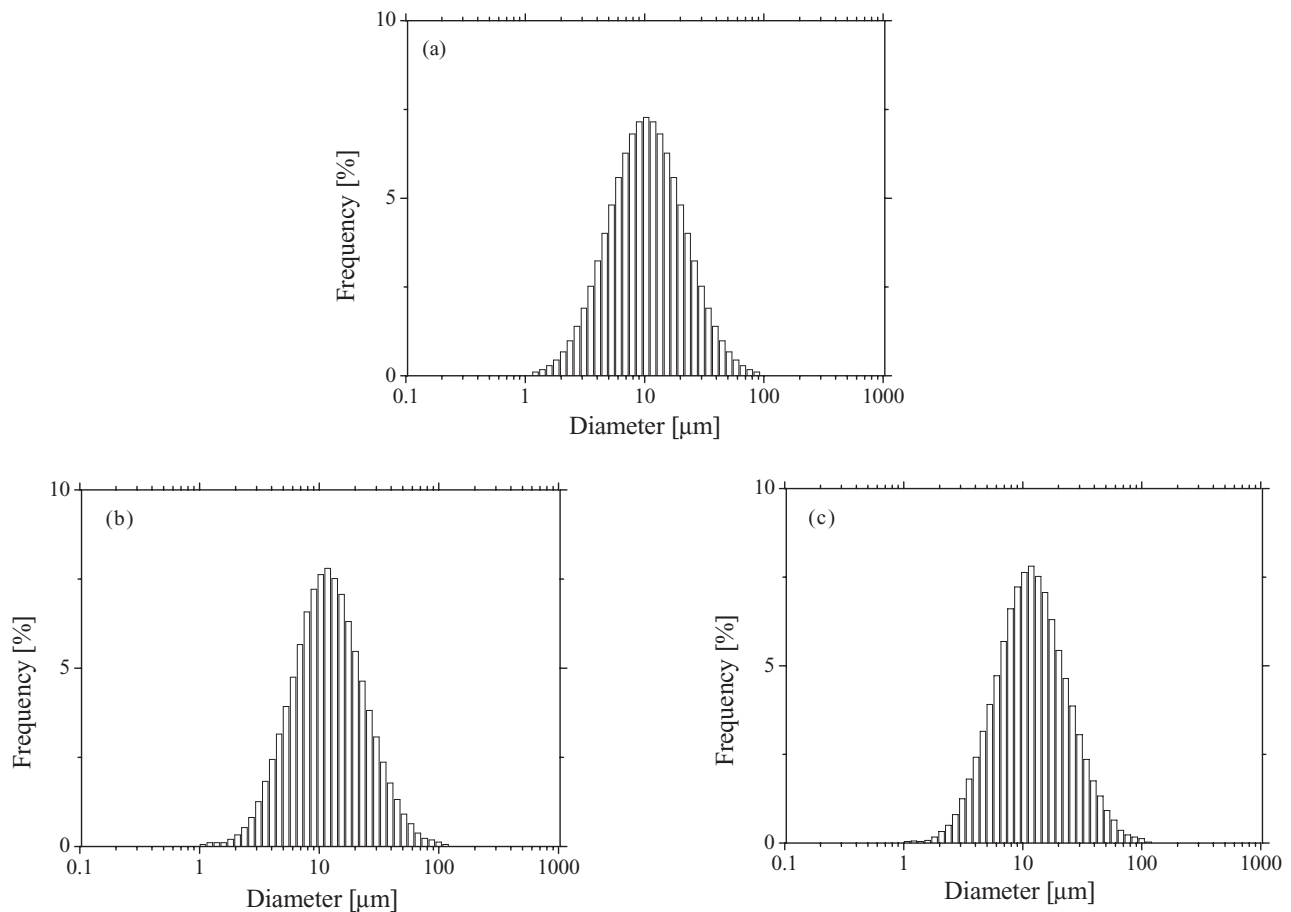


FIG. 6. Comparison of simulated inversed particle size distributions from poly-dispersion (a) by the MT method (b) and by the conventional method (c).

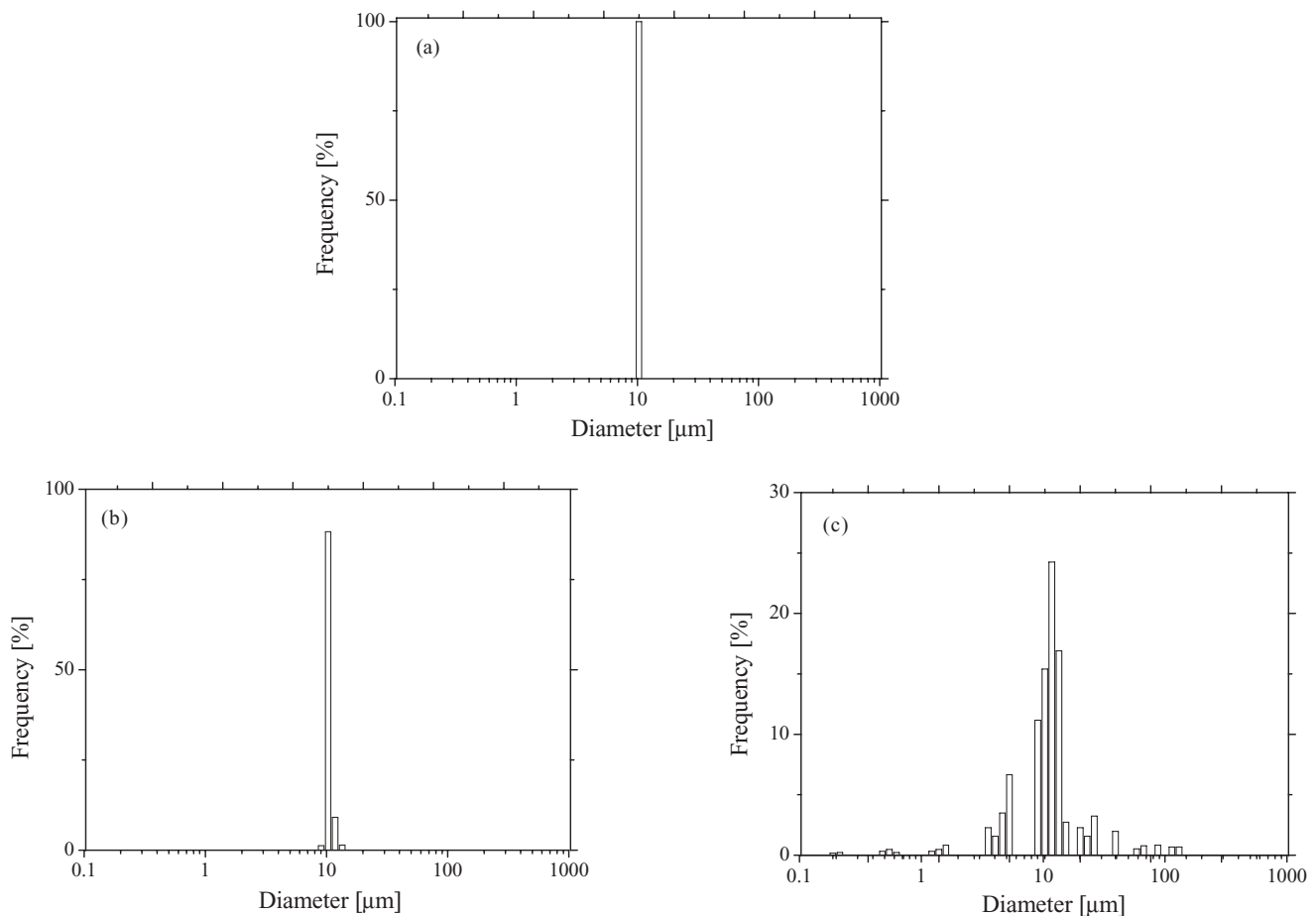


FIG. 7. Comparison of simulated inversed particle size distributions from mono-dispersion (a) by the MT method (b) and by the conventional method (c).

distribution calculated by the MT method, with the detector output calculated from the distribution. The MT method yielded a mean diameter of  $11.6 \mu\text{m}$ . Figure 6(c) shows that the conventional method yielded a mean diameter of  $11.6 \mu\text{m}$ . It is found that both methods agree very closely with each other.

Polystyrene latex is often used as a standard substance as the basis for evaluating the performance of analytical equipment. For this purpose, we shall assume a monodisperse distribution with a mean diameter of  $10.1 \mu\text{m}$ . Figures 7(b) and 7(c), as in Fig. 6 above, show the results obtained for the MT method and the conventional method. The MT method yielded a mean diameter of  $10.2 \mu\text{m}$  and a  $\sigma$  of  $5.1 \times 10^{-4}$ . This is extremely close to the values of the assumed distribution, as shown in Fig. 7(a). On the other hand, the results of the conventional method deviated significantly from the assumed distribution, yielding a broad distribution with a mean diameter of  $10.6 \mu\text{m}$  and a  $\sigma$  of  $1.1 \times 10^{-1}$ . A negative value was obtained, and as this has no physical meaning for the purposes of analysis, the distribution is expressed as zero.

We assume a bimodal distribution composed of a mixture of two monodisperse distributions with peak 1 and peak 2 mean diameters of  $0.584$  and  $6.72 \mu\text{m}$ , respectively, as shown in Fig. 8(a). Figures 8(b) and 8(c) show results obtained for the MT method and the conventional method. The MT method yielded a mean diameter of peak 1 of  $0.584 \mu\text{m}$  and of peak 2 of  $6.72 \mu\text{m}$ . These results show extremely

close agreement with the assumed values and also that the MT method has the requisite reproducibility to deal with multiple-substance distributions. On the other hand, the conventional method did not yield a dual composition distribution.

The detailed results we have obtained are shown in Table I. First, for the assumed values of the polydisperse distribution (i.e., a mean diameter of  $11.6 \mu\text{m}$ ), the value obtained by the MT method was  $11.6 \mu\text{m}$  and that by the conventional method was  $11.6 \mu\text{m}$ . This shows that both methods have good reproducibility. For the value of  $R^2$ , the results obtained by the conventional method appeared to be better at first glance than those given by the MT method by four orders.

TABLE I. Evaluation of the value for particle size distribution  $f(D_j)$  obtained by the MT method and by the conventional method with monodisperse and polydisperse particle size.

Polydisperse	MT method	Conventional method	Assumed values
Mean diameter/ $\mu\text{m}$	11.6	11.6	11.6
Standard deviation/ $\mu\text{m}$	0.10	0.095	0.10
Residue square $R^2$	$6.80 \times 10^{-5}$	$8.40 \times 10^{-9}$	...
Mono-dispersion			
Mean diameter/ $\mu\text{m}$	10.2	10.6	10.1
Standard deviation/ $\mu\text{m}$	$5.1 \times 10^{-4}$	0.11	0
Residue square $R^2$	$3.70 \times 10^{-4}$	0.24	...



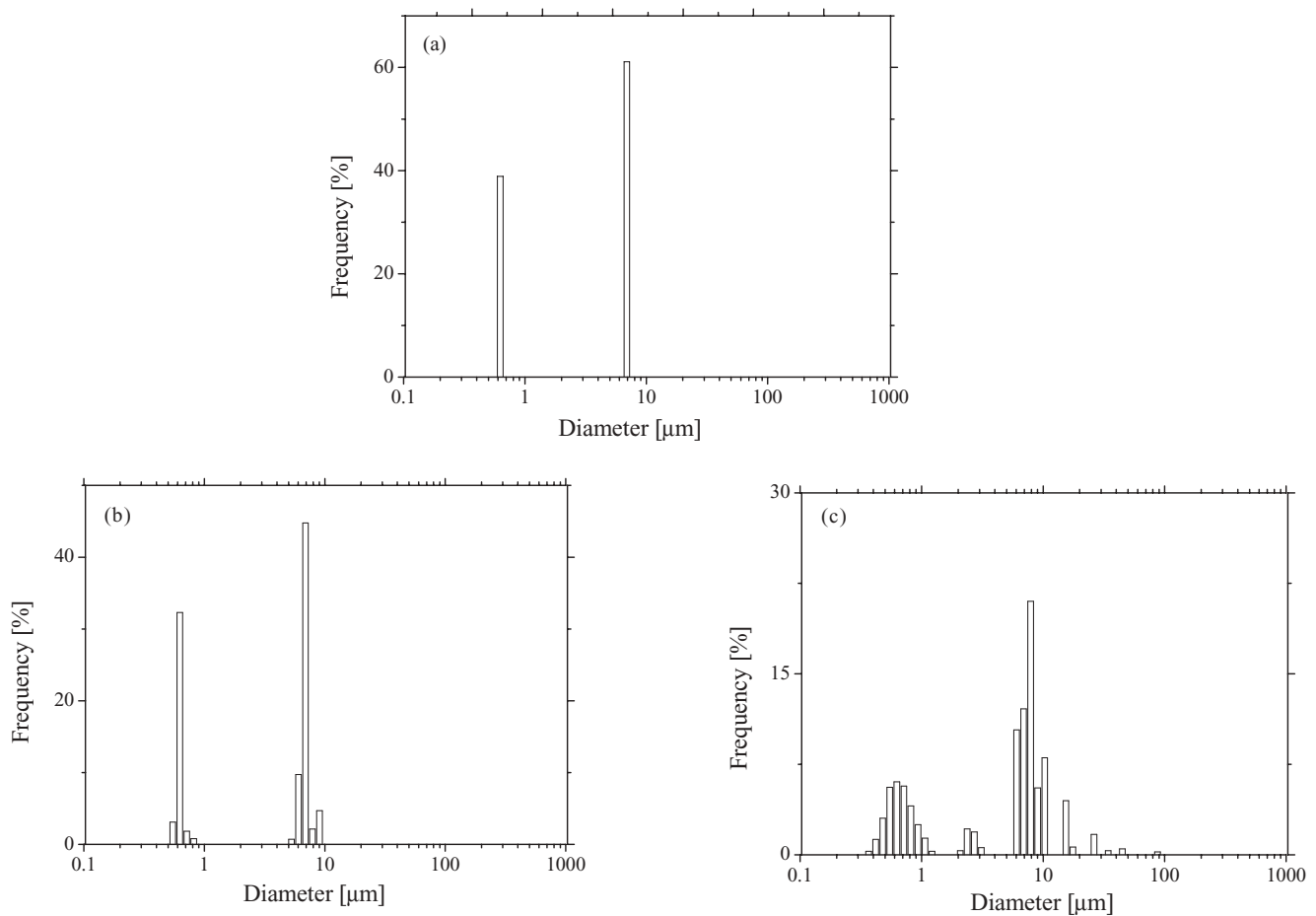


FIG. 8. Comparison of simulated inversed particle size distributions from bimodal mono-dispersion (a) by the MT method (b) and by the conventional method (c).

However, as was seen in Fig. 6, as both methods exhibit essentially identical distribution values for the distribution configuration, a difference less than four order can be considered negligible.

Next, for the assumed values of the monodisperse distribution (i.e., a mean diameter of  $10.1 \mu\text{m}$ ), as was shown in Fig. 7, neither the value obtained by the MT method ( $10.2 \mu\text{m}$ ) nor that obtained by the conventional method ( $10.6 \mu\text{m}$ ) showed any significant deviation from the posited values for the distribution. However, the value of  $\sigma$  of  $5.1 \times 10^{-4}$  yielded by the MT method and that of  $1.1 \times 10^{-1}$  yielded by the conventional method show a difference exceeding two orders of magnitudes and indicate a lack of consistency. Moreover, for residue square  $R^2$ , which expresses the configuration of the distribution, the value given by the MT method was lower than that of the conventional method by less than three orders and expressed the actual distribution quite accurately. Consequently, it can be seen that the MT method yields good reproducibility for both monodisperse and polydisperse distributions. Although the results of the conventional method were good for polydisperse distributions, they were inferior to the MT method for monodisperse distributions.

Table II shows the results of the bimodal distribution composed of a mixture of two monodisperse distributions with peak 1 and peak 2 mean diameters of  $0.669$  and  $6.72 \mu\text{m}$ ,

respectively. The MT method yielded mean diameter of peak 1 of  $0.671 \mu\text{m}$  and of peak 2 of  $7.74 \mu\text{m}$ . These results agree with the assumed values of the distributions. As shown in Fig. 8, while strictly speaking the conventional method did not yield results that permitted a distinction between the two distributions, we approximated the calculations of the mean diameter and the  $\sigma$  assuming a dual composition distribution. These calculations yielded a mean diameter of  $0.727 \mu\text{m}$  for peak 1 and of  $7.66 \mu\text{m}$  for peak 2. For  $\sigma$  of the bimodal case, the MT method yielded values of  $1.9 \times 10^{-4}$  for peak 1 and  $6.6 \times 10^{-1}$  for peak 2. The conventional method yielded  $3.5 \times 10^{-2}$  for peak 1 and  $3.0$  for peak 2 with poor consistency and reproducibility. For the value of  $R^2$ , the result obtained by the conventional method was  $1.3 \times 10^{-2}$ , a

TABLE II. Evaluation of the value for bimodal particle size distribution  $f(D_j)$  obtained by the MT method and by the conventional method.

		MT method	Conventional method	Assumed values
Mean diameter/ $\mu\text{m}$	Peak 1	0.671	0.727	0.669
	Peak 2	7.74	7.66	6.72
Standard deviation/ $\mu\text{m}$	Peak 1	$1.9 \times 10^{-3}$	$3.5 \times 10^{-2}$	0
	Peak 2	$6.6 \times 10^{-1}$	3.0	0
Residue square $R^2$		$3.70 \times 10^{-4}$	$1.30 \times 10^{-2}$	...

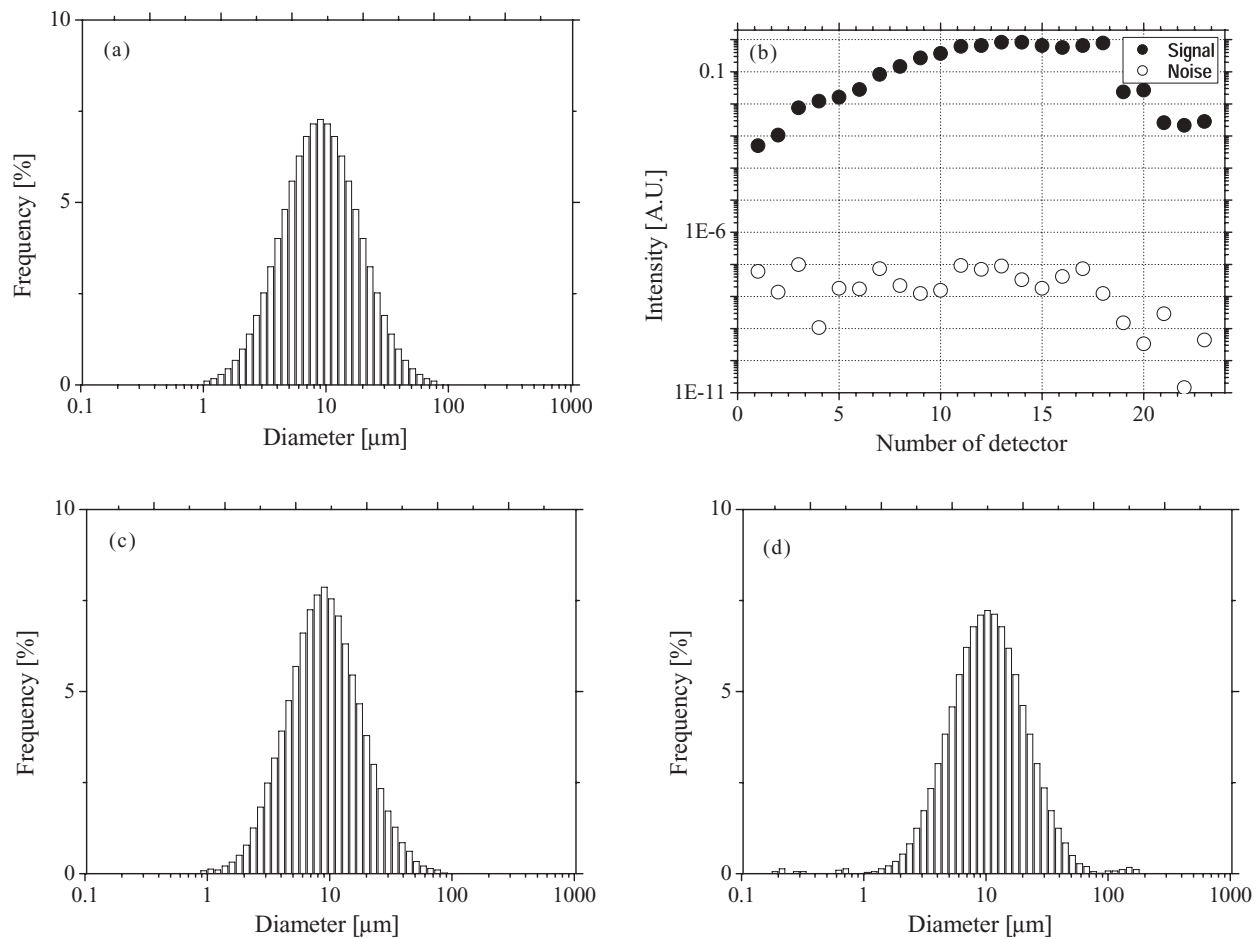


FIG. 9. Comparison of noise effect in the case of polydispersed particle size distribution (a) by the MT method (c) and by the conventional method (d). The scattering intensities from assumed poly-distribution are shown (b) by symbol (●) and noise intensities are shown by symbol (○).

value larger by two orders, than  $3.7 \times 10^{-4}$  given by the MT method.

Figure 8 clearly shows that the distribution configuration given by the conventional method is a poor representation. Therefore, it is found that the MT method exhibits good reproducibility for the complex distribution of samples composed of multiple substances.

Next, we investigated the effect of noise on the particle size distribution. As shown Fig. 9(a), we first assume a poly-disperse particle size distribution with a mean diameter of  $8.82 \mu\text{m}$  and a  $\sigma$  of  $1.2 \times 10^{-1}$ . We can then calculate the detector output, and Fig. 9(b), we add the noise that is estimated to be generated by the type of detector we used. A typical optical noise observed by a Horiba Laser light scattering particle size distribution analyzer (LA-910) was used for the simulation. Figures 9(c) and 9(d) show the results obtained from this by the MT method and the conventional method. The results are similar to those shown in Fig. 6. The MT method yielded a mean diameter of  $8.75 \mu\text{m}$  and a  $\sigma$  of  $9.5 \times 10^{-2}$ , which agree well with the particle size distribution values without noise. The results of the conventional method showed a mean diameter of  $9.34 \mu\text{m}$  and a  $\sigma$  of  $1.1 \times 10^{-1}$ , agreeing with the assumed values for the distribution. However, in the case of the conventional method, the effect of the added noise was to cause the appearance of ghost peaks,

particle diameters where there should have been no distribution. In addition, minus values appeared sporadically (these are expressed as zero). For the value of  $R^2$ , the result from the MT method was  $4.8 \times 10^{-3}$  and result from the conventional method was  $1.6 \times 10^{-3}$ , showing that for polydisperse distributions, there is no significant difference between the results of the MT method and the conventional method. In Fig. 10, just as in Fig. 9, part (a) shows the assumed distribution, this time for a monodisperse distribution. Here, we posit a mean diameter of  $10.1 \mu\text{m}$ . Figures 10(c) and 10(d) show the results obtained from scattering intensities in Fig. 10(b) by the MT method and the conventional method. The MT method yielded a mean diameter of  $9.92 \mu\text{m}$  and a  $\sigma$  of  $4.8 \times 10^{-4}$ . This agrees with the particle size distribution values obtained previously without noise. The results of the conventional method, on the other hand, deviated significantly: a  $10.2 \mu\text{m}$  mean diameter and a  $\sigma$  of  $1.2 \times 10^{-1}$ . In addition, ghost peaks appeared. For the value of  $R^2$ , the result obtained by the MT method was  $5.1 \times 10^{-4}$  and by the conventional method was  $6.2 \times 10^{-2}$ . The MT method is superior to the conventional method with regard to reproducibility for monodisperse distributions.

Up to this point, we have presented individual examples for distributions. Next, we simulated particle size distributions for the overall diameter. Figure 11 shows the  $R^2$  result

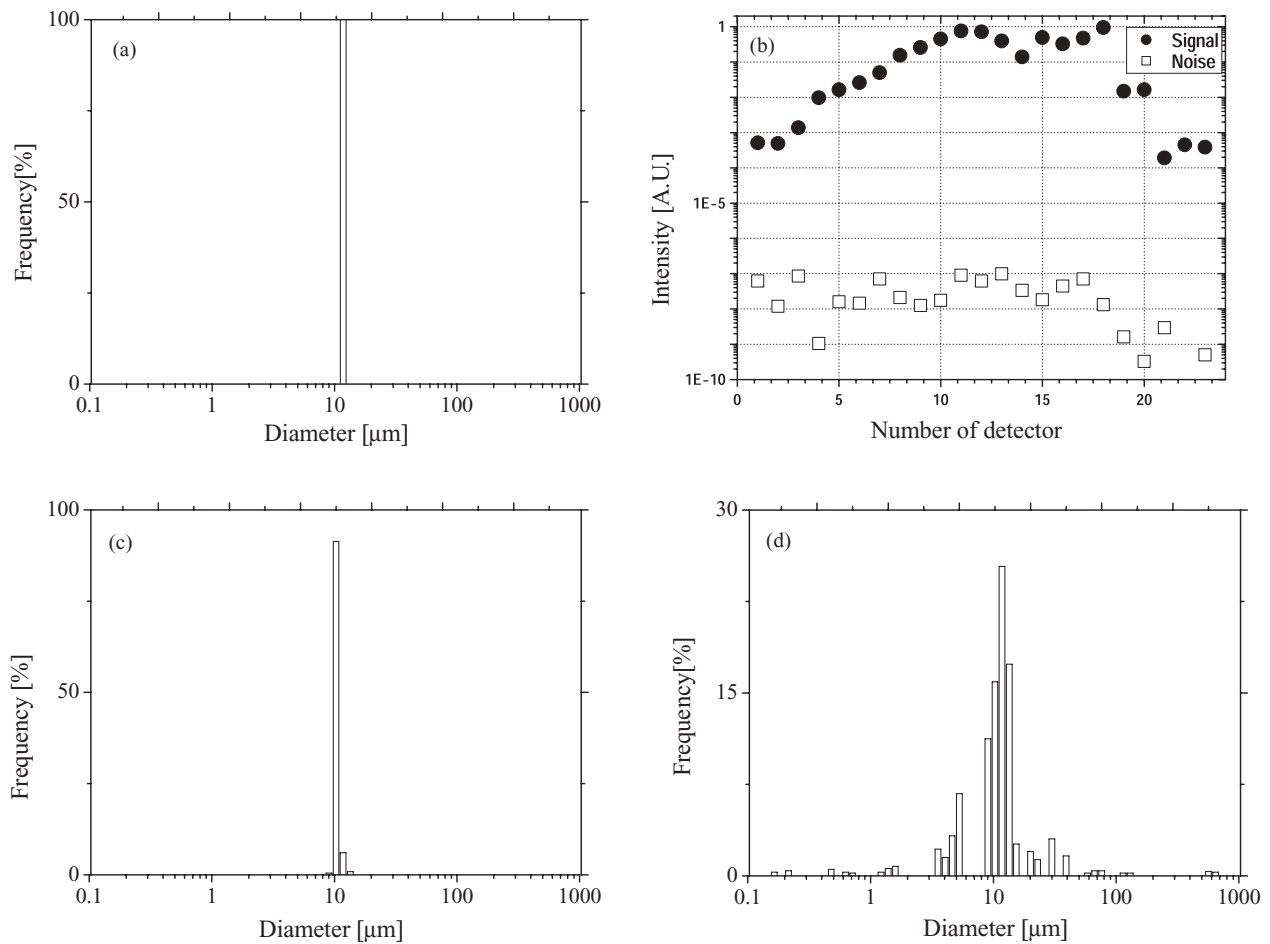


FIG. 10. Comparison of noise effect in the case of monodispersed particle size distribution (a) by the MT method (c) and by the conventional method (d). The scattering intensities from assumed mono-distribution are shown (b) by symbol (●) and noise intensities are shown by symbol (○).

obtained for a polydisperse distribution with the assumed mean diameter in the range of  $0.5\text{--}200\ \mu\text{m}$ . Here, the value of  $R^2$  obtained from both the MT and the conventional method were of the order of  $10^{-3}$  for a mean diameter of any size within the range. This indicates that there is no significant difference between the two methods, whether for the particle size distribution or for reproducibility.

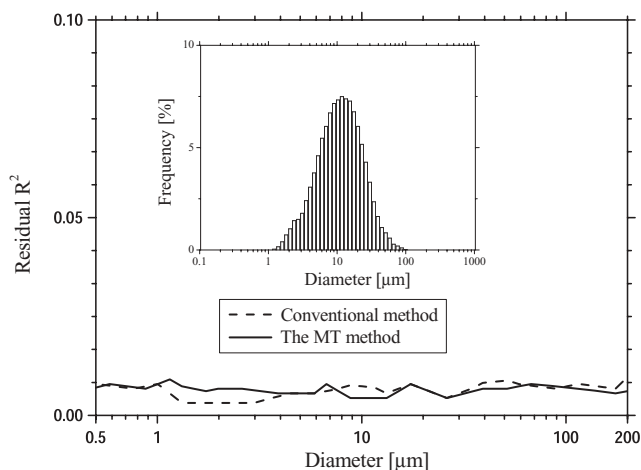


FIG. 11. Value of residual  $R^2$  vs particles size in the case of polydisperse particle size included in the noise signals.

Figure 12 shows the variation in  $R^2$  obtained for a monodisperse distribution with the assumed range of mean diameters in the range of  $0.1\text{--}1000\ \mu\text{m}$ . The MT method consistently yielded a value of  $R^2$  of the order of  $10^{-2}$  to  $10^{-3}$ , for all particle diameters within the range. However, the value of  $R^2$  by the conventional method was 100 times as large as

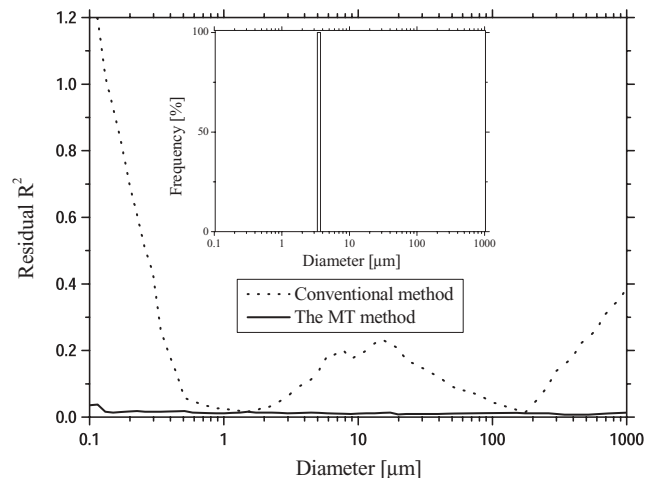


FIG. 12. Value of residual  $R^2$  vs particles size in the case of monodisperse particle size included in the noise signals.



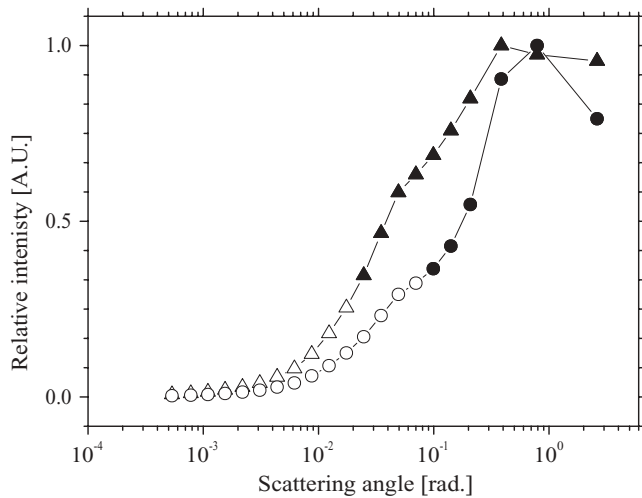


FIG. 13. Normalized scattering patterns that are used for the MT method. Monoparticle size distribution ( $\circ$ ) and polyparticle size distribution ( $\Delta$ ) results at relative refractive index 1.3 with 633 nm. Filled symbols ( $\bullet$ ) and ( $\blacktriangle$ ) show detectors, which are more than 0.3 of scattering intensity.

the MT method at the less than 0.5 mm and 100 mm or less. This showed that the conventional method used here was extremely susceptible to the effects of noise in the distribution configuration and had poor reproducibility. Low susceptibility to noise in the distribution configuration makes the MT method an effective analytic tool.

The conventional and the MT methods show good inverted results for distributed particle size data as shown in Fig. 11. On the other hand,  $R^2$  data show a difference between the MT method and the conventional method, as highlighted in Fig. 12, at monodisperse particle size.

The kernel function  $K_i(D_j)$  in the MT method plays an important part in stabilizing the results of  $R^2$  between monodisperse and polydisperse particle size distributions. When the width of the particle size distribution is decreased, scattering signals are localized to specified detectors. When other detectors receive fewer signals, the signal-to-noise is increased, and the difference between the calculated and actual signal ( $Kf-g$ ) is decreased. Therefore, the solution is unstable under the conditions of the conventional method. The kernel function used in the MT method is also a weighted function in the calculation. The weighting function stabilizes the results even if the differences are small.

We expect the MT method shows more stable results than the conventional method when a number of effective detectors is limited. The relative intensities of signals themselves have a function of weighted parameters in the MT method. Examples of scattering patterns with mono- and poly-distribution are shown in Fig. 13. Monoparticle size distribution shows a narrower scattering profile than the polydispersed pattern. If the effective relative signal intensity is more than 0.3, the number of effective detectors is six of 24 at a narrow particle size distribution. In contrast, the number of effective detectors is 10 of 24 at wider particle size distribution. When the width of the particle size is changed, the number of effective detectors is also changed. When the particle size distribution is narrower, the number of effective detectors is smaller. We

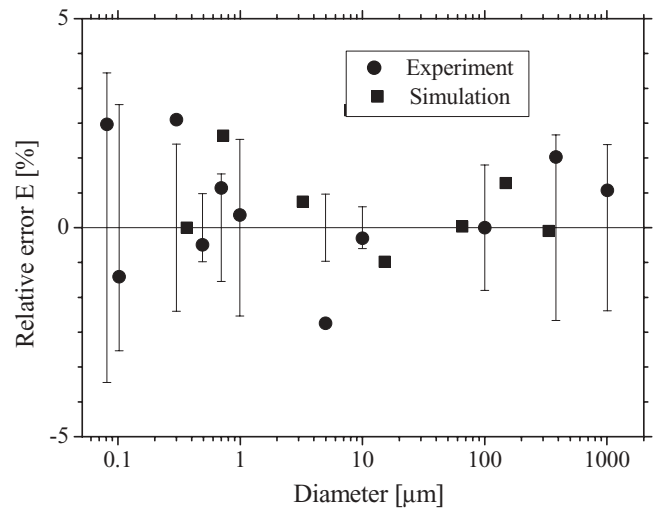


FIG. 14. An example of relative error obtained by experimental and simulated results of monodisperse particle size. Bar shows uncertain range of samples.

expect that a smaller number of detectors are less affected by noise than a larger number of detectors.

## VII. THE EXPERIMENTAL METHOD

Eleven monodispersed polystyrene latexes (4000 and 5000 series; Thermo Fisher Scientific Inc.) were used to test the inverse of mono-distributions. The mean diameters of the latex were 0.081, 0.102, 0.300, 0.491, 0.701, 0.993, 4.991, 9.975, 100.0, 383.0, and 1007  $\mu\text{m}$  with size fluctuations within 0.5%–3.7% of the nominal diameters as stated by the manufacturer. The relative refractive index of polystyrene is 1.19 when water is used. All samples are diluted by de ionized water so that transmitted percent might become 90 to 95. All samples were measured by a Horiba Laser light scattering particle size distribution analyzer (LA-910) with the MT method. The relative error is defined as

$$E = \frac{D_r - D_c}{D_c} \times 100(\%), \quad (10)$$

where  $D_r$  is the measured particle size and  $D_c$  is the certified particle size.

The inversed mean diameters of experimental results are shown in Fig. 14 for all studied samples. All samples of mean size were consistent with nominal size within 3% accuracy. Except for 0.300 and 4.991  $\mu\text{m}$  particles, inverted mean sizes agreed with the nominal size to be within the range of 0.5%–3.7% size uniformity of these samples.

## VIII. CONCLUSION

In this paper, a new iteration method for LALLS, which has a simple algorithm and no restricted condition between the number of detectors and column of diameters, was presented. The iteration method is based on the Twomey method. New weighting functions, which are related nominal and speed of convergence, are introduced to the Twomey method. The weighted functions in the iteration algorithm are a very

important feature in stabilizing the convergence speed in the algorithm. It was shown that the MT method requires no special parameters, conditions, or assumptions to obtain the particle size distribution. The MT method showed reliable results for the narrow size distribution as compared with the conventional method. Moreover, the MT method was more resistant to the effects of noise than conventional method at narrow size distribution. The results of wider size distribution also showed reliable results, which were similar to the conventional method.

<sup>1</sup>R. H. Muller and W. Mehnertm, *Particle and Surface Characterization Methods* (Medpharm Scientific Publishers, Stuttgart, 1997), Chaps. 2–4.

<sup>2</sup>R. Xu, *Particle Characterization* (Kluwer Academic Publishers, Dordrecht, 2000), Chap. 2.

<sup>3</sup>*Particle Size Distribution III*, ACS Symposium Series 693, edited by T. Prorder (Oxford University Press, Oxford, 1998), Chap. 10.

<sup>4</sup>Y. Wei, B. Ge, and Y. Wei, *Appl. Opt.* **48**, 1779 (2009).

<sup>5</sup>V. P. Maltsev and V. N. Lopatin, *Appl. Opt.* **36**, 6102 (1997).

<sup>6</sup>U. Anato, D. D. Bello, F. Esposito, C. Serio, G. Pavese, and F. Romano, *J. Geophys. Res.* **101**, 19267 (1996).

<sup>7</sup>Z. Cao, L. Xu, and J. Ding, *Appl. Opt.* **48**, 4842 (2009).

<sup>8</sup>R. Xu, *Particle Characterization* (Kluwer Academic Publishers, Dordrecht, 2000), Chap. 3.

<sup>9</sup>S. Twomey, *J. Comput. Phys.* **18**, 188 (1975).

<sup>10</sup>A. Bassini, S. Musazzi, E. Paganini, U. Perini, F. Ferri, and M. Giglio, *Opt. Eng.* **31**, 1112 (1992).

<sup>11</sup>F. Ferri, M. Giglio, and U. Perini, *Appl. Opt.* **28**, 3074 (1989).

<sup>12</sup>G. J. Sem, J. K. Agarwal, and C. E. McManns, EPA-600/9-80-004 (1997), pp. 276–301.

<sup>13</sup>J. Zhou, F. Moshary, B. Gross, and S. Ahmed, *Appl. Opt.* **45**, 6876 (2006).

<sup>14</sup>H. Yoshida, H. Masuda, K. Fukui, and Y. Yokunaga, *Adv. Powder Technol.* **12**, 79 (2001).

<sup>15</sup>R. M. Vanck, H. Luck, and N. G. Bernigau, *AEROSOLS, Proceedings of the Third International Aerosol Conference*, Kyoto, 1990.

<sup>16</sup>A. Boxman, H. G. Merkus, P. J. Verheijen, and B. Scarlett, *Appl. Opt.* **30**, 4818 (1991).

<sup>17</sup>W. Jianping, X. Shizhong, Z. Yimo, and L. Wei, *Appl. Opt.* **40**, 3937 (2001).

<sup>18</sup>L. P. Bayvel and A. R. Johns, *Electromagnetic Scattering and its Applications* (Applied Science Publishers, Essex, 1981), Chap. 1.

<sup>19</sup>C. F. Bohren and D. R. Huffman, *Absorption and Scattering of Light by Small Particles* (Wiley, New York, 1983), Chap. 4.

<sup>20</sup>M. Kerker, *The Scattering of Light and Other Electromagnetic Radiation* (Academic, New York, 1969), Chap. 4.4.